



Binuclear copper(II) complexes **1**: Synthesis, characterization and evaluation of a new complex in phosphatase-like activity

Olivier Schicke^a, Bruno Faure^a, Michel Giorgi^b, A. Jalila Simaan^a, Marius Réglier^{a,*}

^aInstitut des Sciences Moléculaires de Marseille/Biosciences UMR CNRS 7313, Aix-Marseille Université, Campus Scientifique de St-Jérôme, avenue Escadrille Normandie-Niemen, 13397 Marseille Cedex 20, France

^bSpectropole FR CNRS 1739, Aix-Marseille Université, Campus Scientifique de St-Jérôme, avenue Escadrille Normandie-Niemen, 13397 Marseille Cedex 20, France

ARTICLE INFO

Article history:

Received 20 January 2012

Received in revised form 11 April 2012

Accepted 11 April 2012

Available online 3 May 2012

Keywords:

Copper

Binuclear copper(II) complex

Phosphatase-like activity

ABSTRACT

A new binuclear Cu(II) complex derived from a pamoic type ligand has been synthesized and characterized by X-ray crystallography. This complex was checked as catalysts in the hydrolysis of bis(*p*-nitrophenyl)phosphate. Its catalytic properties were studied at various pH and compared to the mononuclear Cu(II) complex. At pH 5.38, the binuclear Cu(II) complex exhibited a phosphatase-like activity with 11 TON and 24% conversion and was found to be 41-fold more active than the mononuclear counterpart.

© 2012 Elsevier B.V. All rights reserved.

1. Introduction

The development of dinuclear metal ion complexes that promote the hydrolysis of phosphate ester linkages has been a subject of great interest during the last decade [1,2]. On one hand, the design of functional models for hydrolytic metalloenzymes that contain two metal ion in their active site [3–5] is of great importance in biotechnology for the prospect of synthetic nucleases which could be used as artificial restriction enzymes [6]. On the other hand, since a number of phosphate esters and related P(V) compounds are used in agriculture as pesticides or, unfortunately, as potent nerve agents in chemical weapons, the development of catalytic systems able to hydrolyze and destroy such compounds is of considerable environmental and medicinal importance. Due to its high natural abundance and good Lewis acid properties, Mg(II) is the most important metal encountered in nucleases [7], but multinuclear transition metal centers with Zn(II), Mn(II) and Fe(II/III) are often present too [3]. In these binuclear systems, hydrolysis occurs generally by a double Lewis acid activation: one of the metal ions renders the coordinated water more acidic while the second metal activates the phosphate ester group thus favoring an intramolecular hydrolysis of the phosphoester group (Scheme 1).

Nuclease mimics incorporating a dinuclear metal center with Co [8,9], Ln [10–12], Zn [13–15], and Fe [16] were recently published as bioinspired efficient catalysts in phosphoester hydrolysis. While Cu(II) has never been identified as cofactor in natural nucleases,

this metal exhibits interesting features rendering it attractive for artificial nucleases: (i) Cu(II) is substitutionally labile and at the same time a strong Lewis acid necessary for activation of the phosphodiester bond via nucleophilic attack and (ii) Cu(II) lowers the pK_a of coordinated water, thereby providing metal-bound hydroxide at near-neutral pH. That is the reason why binuclear Cu(II) complexes have also been described as efficient catalysts in phosphoester hydrolysis [17–23]. We report on the synthesis and the characterization of a new binuclear copper(II) complex based on a pamoic moiety which exhibit a remarkable catalytic phosphatase-like activity compared to mononuclear copper(II) complexes.

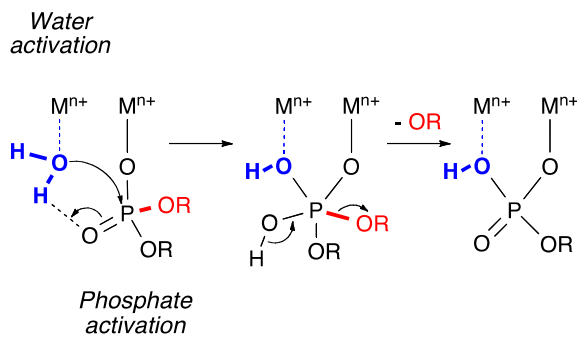
2. Experimental

2.1. General

All chemicals were obtained from commercial sources and used as received. THF and dichloromethane were respectively distilled from sodium-benzophenone and calcium hydride. Silica gel TLC and column chromatography were performed using Meck Kieselgel 60F₂₅₄ and silica gel 60 (0.063–0.200). Each compound which mass spectrometry data is given had its structure confirmed by (ESI)MS/MS. All NMR spectra were recorded with Bruker Avance DPX200 and DPX300 using TMS as internal reference. X-band ESR spectra were obtained using a BRUKER EMX9/2.7 spectrometer equipped with a B-VT2000 digital temperature controller (100–400 K). The simulations with automatic parameter fitting were performed for axial symmetry [24]. The contribution of naturally abundant ⁶³Cu

* Corresponding author. Tel.: +33 4 91 28 8823; fax: +33 4 91 28 8440.

E-mail address: marius.reglier@univ-amu.fr (M. Réglier).



and ^{65}Cu was considered, but the values given in the text refer to ^{63}Cu . All principal axes were supposed parallel.

2.2. Methyl pamoate, **1**

Methyl pamoate **1** was synthesized starting from the commercially available pamoic acid according to a literature procedure [25]. Recrystallization in methanol affords compound **1** as white crystals. Crystal data for compound **1**, together with details of the single crystal X-ray diffraction experiment are reported in Table 1 and an ORTEP representation in Fig. 1A.

2.3. Methyl 2,2'-[1,2-ethanediylbis(oxy)]-1,1'-dinaphthylmethane-3,3'-dicarboxylate, **2**

To a stirred solution of methyl pamoate **1** (1.1 g, 2.64 mmol) in dry acetone (500 cm³) was successively added anhydrous potassium carbonate (2.92 g, 21.1 mmol) and 1,2-dibromoethane (0.22 cm³, 2.64 mmol). The suspension was stirred and refluxed for a week, then vacuum evaporated. The solid obtained was dissolved in 50 cm³ dichloromethane and washed several times with distilled water. The organic phase was dried over MgSO₄, and vacuum evaporated. Purification was done by fractional crystallization removal of product **1** using ethyl acetate (or chloroform) as solvent to afford a white solid (0.16 g, 14%); mp 211 °C; $\nu_{\text{max}}/\text{cm}^{-1}$ 2941 (CH), 1718 (CO), 1622 and 1589 (C–Carom), 1190 and 1148 (CO); δ_{H} (300 MHz, CDCl₃, Me₄Si) 3.92 (6H, s, OCH₃), 4.50 (4H, m, OCH₂–CH₂O), 5.09 (2H, s, naph-CH₂-naph), 7.45 (4H, m, naph), 7.86 (2H, d, $J = 7.80$, naph), 8.08 (2H, d, $J = 7.97$, naph), 8.29 (2H, s, naph) ppm; δ_{C} (75.47 MHz, CDCl₃, Me₄Si) 20.50, 52.65, 75.08,

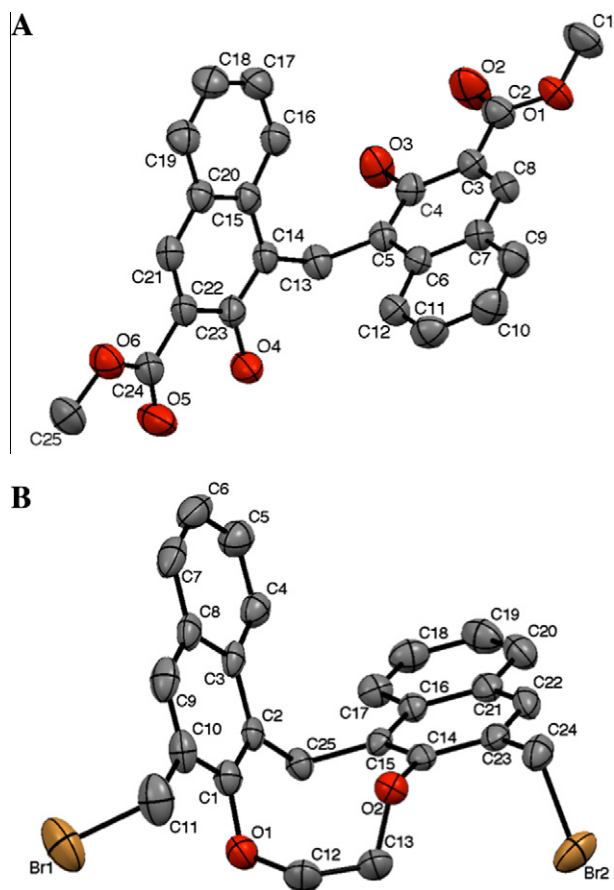


Fig. 1. ORTEP drawings of (A) and **4** (B) (displacement ellipsoids are drawn at 50% probability level).

123.50, 124.01, 125.19, 128.63, 129.64, 129.98, 131.74, 134.59, 154.83, 166.48 ppm; MS m/z (ESI): 443 [M+H⁺].

2.4. 2,2'-[1,2-Ethanediylbis(oxy)]-1,1'-dinaphthylmethane-3,3'-methyl alcohol, **3**

A solution of **2** (0.090 g, 0.2 mmol) in THF (5 cm³) was added cautiously to a stirred suspension of lithium aluminum hydride (0.190 g, 5 mmol) in THF (10 cm³). After 3 h of reaction the mixture

Table 1
Crystal data for the compounds **1**, **4**, **6** and **7**.

	1	4	6	7
Formula	C ₂₅ H ₂₀ O ₆	C ₂₅ H ₂₀ Br ₂ O ₂	C ₅₆ H ₅₈ Cu ₂ F ₁₂ N ₆ O ₁₉ S ₄	C ₂₃ H ₂₄ CuF ₆ N ₄ O ₇ S ₂
M _w	416.41	512.23	1600.45	710.12
Crystal system	orthorhombic	monoclinic	monoclinic	monoclinic
Space group	<i>Pbcn</i>	<i>P2₁/c</i>	<i>P2₁/c</i>	<i>P2₁</i>
<i>a</i> (Å)	10.3290(7)	4.8000(2)	18.3967(1)	11.0690(6)
<i>b</i> (Å)	14.7250(9)	23.571(2)	13.8680(1)	8.641(7)
<i>c</i> (Å)	26.376(1)	18.571(2)	26.5326(2)	16.481(1)
β (°)	90	101.927(5)	98.1940(4)	108.812(2)
<i>V</i> (Å ³)	4011.6(4)	2055.8(3)	6700.04(8)	1492(1)
<i>Z</i>	8	4	4	2
μ (Mo K α) (mm ⁻¹)	0.099	3.962	0.867	0.957
Unique reflections, <i>R</i> _{int}	4792, 0.076	3780, 0.108	11369, 0.053	2880, 0.040
Reflections with <i>I</i> > 2(<i>I</i>)	3211	2677	9472	2659
Final <i>R</i> indices for <i>I</i> > 2(<i>I</i>)	<i>R</i> = 0.066	<i>R</i> = 0.061	<i>R</i> = 0.0648	<i>R</i> = 0.039
	<i>wR</i> = 0.116	<i>wR</i> = 0.096	<i>wR</i> = 0.1712	<i>wR</i> = 0.088
<i>R</i> indices (all data)	<i>R</i> = 0.109	<i>R</i> = 0.097	<i>R</i> = 0.0782	<i>R</i> = 0.045
	<i>wR</i> = 0.134	<i>wR</i> = 0.1102	<i>wR</i> = 0.1815	<i>wR</i> = 0.093
Flack parameter				0.074(18)

was hydrolyzed by successive addition of distilled water (0.190 cm³), NaOH 1 M (0.380 cm³), then distilled water (0.190 cm³) and left under stirring for 1 h. The reaction mixture was centrifuged, the supernatant dried through a microcolumn of anhydrous Na₂SO₄. Vacuum evaporation of THF affords compound **3** as a white solid (0.075 g, 98%); mp 293 °C; $\nu_{\max}/\text{cm}^{-1}$ 3342 (OH), 2954 (CH), 1624 and 1598 (C–Carom), 1192 (CO); δ_{H} (200 MHz, DMSO, Me₄Si) 4.36 (4H, m, OCH₂–CH₂O), 4.65 (4H, s, CH₂OH), 4.98 (2H, s, naph-CH₂-naph), 5.22 (2H, s, OH), 7.38 (4H, m, naph), 7.81 (2H, s, naph), 7.87 (2H, m, naph), 8.13 (2H, m, naph) ppm; δ_{C} (50.32 MHz, DMSO, Me₄Si) 22.40, 58.55, 73.19, 123.31, 124.31, 125.11, 125.74, 127.38, 128.35, 130.48, 131.47, 135.03, 154.20 ppm.

2.5. 2,2'-[1,2-Ethanediybis(oxy)]-1,1'-dinaphthylmethane-3,3'-bromomethane, **4**

To a suspension of **3** (0.080 g, 0.21 mmol) in dichloromethane (10 cm³) was added phosphorus tribromide (0.04 cm³, 0.43 mmol) via micro-syringe. The mixture was stirred and refluxed for 24 h. After cooling the solution was washed by a saturated aqueous NaHCO₃ solution (2 × 50 cm³), distilled water (50 cm³) then dried over anhydrous Na₂SO₄. Dichloromethane was vacuum evaporated to give a solid that was purified by column chromatography using diethyl ether as solvent. Compound **4** was recrystallized from chloroform to give white crystals (0.054 g, 51%); mp 235 °C (decomposition); $\nu_{\max}/\text{cm}^{-1}$ 2910 (CH), 1621 and 1595 (C–Carom), 1195 (CO), 700 (CBr); δ_{H} (200 MHz, CDCl₃, Me₄Si) 4.67 (8H, m, CH₂Br and OCH₂–CH₂O), 5.03 (2H, s, naph-CH₂-naph), 7.38 (4H, m, naph), 7.78 (2H, m, naph), 7.81 (2H, s, naph), 8.03 (2H, m, H8) ppm; δ_{C} (50.32 MHz, CDCl₃, Me₄Si) 23.73, 29.15, 74.41, 123.54, 124.98, 127.20, 128.56, 128.88, 129.91, 130.65, 130.98, 133.25, 154.68 ppm; MS *m/z* (ESI): 513[M+H⁺], 511 (51%), 515 (48%). Crystal data for compound **4**, together with details of the single crystal X-ray diffraction experiment are reported in Table 1 and an ORTEP representation in Fig. 1B.

2.6. N,N,N-Bis(2-picolyl)-(2,2'-[1,2-ethanediybis(oxy)]-1,1'-dinaphthylmethane-3,3'-methyl) amine, **5**

To a solution of **4** (0.056 g, 0.10 mmol) in ethyl acetate (2 cm³) was successively added a solution of bis(2-picolyl)amine (0.057 cm³) in ethyl acetate (2 cm³), then a solution of *N,N*-diisopropylethylamine (0.025 cm³, 0.21 mmol) in ethyl acetate (2 cm³). The mixture was refluxed under stirring for 15 h. Ethyl acetate was removed by vacuum evaporation. The resulting crude solid was solubilized in dichloromethane (50 cm³), washed successively by distilled water (50 cm³), saturated aqueous NaHCO₃ solution (50 cm³), distilled water (50 cm³) then dried over anhydrous Na₂SO₄. Dichloromethane was vacuum evaporated to give brown product purified by column chromatography using acetone then an acetone/MeOH (95/5) mixture as eluent. Vacuum evaporation affords compound **5** as a white solid (0.035 g, 47%); δ_{H} (200 MHz, acetone-*d*₆, Me₄Si) 3.81 (8H, s, N-CH₂-Pyr × 4), 3.89 (4H, s, naph-CH₂-N), 4.21 and 4.33 (4H, m, O-CH₂-CH₂-O), 5.00 (2H, s, naph-CH₂-naph), 7.13 (4H, m, pyr), 7.30 (4H, m, naph), 7.59 (8H, m, pyr), 7.82 (2H, m, naph), 8.07 (4H, m, naph), 8.44 (4H, m, pyr) ppm; δ_{C} (50.32 MHz, acetone-*d*₆, Me₄Si) 24.92, 55.30, 62.01, 75.57, 123.75, 124.69, 125.41, 126.19, 127.74, 129.94, 130.17, 130.53, 133.02, 133.87, 134.24, 138.04, 150.73, 157.88, 161.16 ppm.

2.7. Binuclear copper(II) complex, **6**

To a stirred solution of compound **5** (0.035 g, 46 μmol) in acetone (5 cm³) was added a solution of copper(II) triflate (0.033 g,

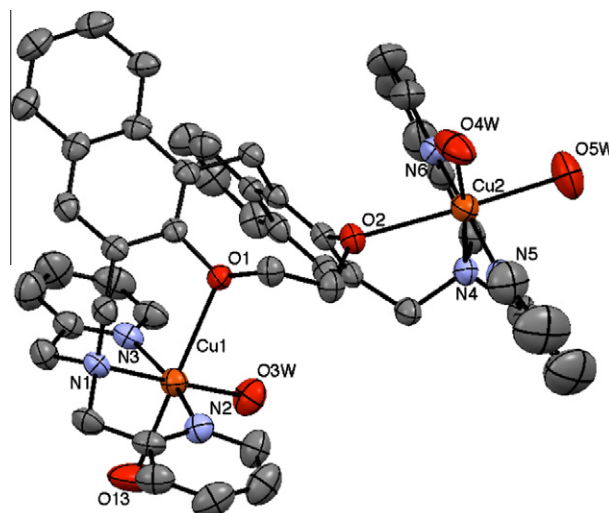


Fig. 2. ORTEP drawings of **6**, the H-atoms and the three un-coordinated triflate counter ions have been removed for clarity (displacement ellipsoids are drawn at the 50% probability level).

93 μmol) in acetone (2 cm³). After 3 h of reaction, precipitation with diethylether affords compound **6** as blue solid (0.034 g). The slow evaporation at room temperature of a saturated acetone solution of compound **6** affords deep blue crystals suitable for a single crystal X-ray analysis. Crystal data for complex **6**, together with details of the X-ray diffraction experiment are reported in Table 1 and an ORTEP representation in Fig. 2. The X-structure reveals the presence of a non-coordinated acetone molecule and four water molecules; mp = 257 °C (decomposition); $\nu_{\max}/\text{cm}^{-1}$ 3429 (OH), 1613 and 1575 (C–Carom), 1222 (CF), 1025 (SO). Elemental Anal. Calc. for C₅₆H₅₈Cu₂F₁₂N₆O₁₉S₄ (MW 1602.42): C, 41.97; H, 3.65; N, 5.24. Found: C, 40.73; H, 3.46; N, 5.39%.

2.8. Mononuclear copper(II) complex, **7**

To a stirred solution of *N*-benzyl-bis-2-picolylamine [26] (0.300 g, 1.03 mmol) in chloroform (10 cm³) was added a solution of copper(II) triflate (0.375 g, 1.03 mmol) in chloroform (10 cm³). After three hours of stirring at room temperature the mixture was precipitated with diethylether and filtered to give a blue solid (0.360 g, 50%). The slow evaporation at room temperature of a sat-

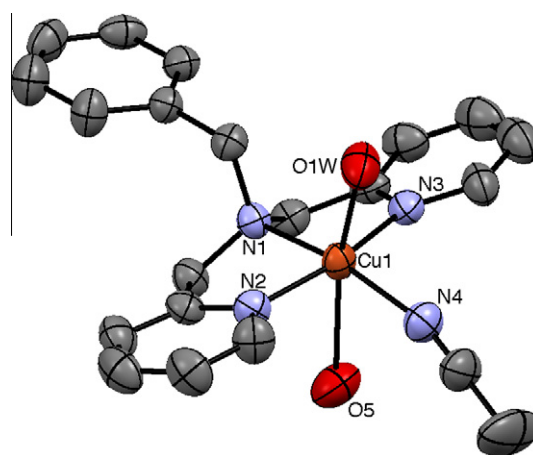


Fig. 3. ORTEP drawings of **7**, the H-atoms and the un-coordinated triflate counter ion has been removed for clarity (displacement ellipsoids are drawn at the 50% probability level).

urated acetonitrile solution of compound **7** affords deep blue crystals suitable for a single crystal X-ray analysis. Crystal data for complex **7**, together with details of the X-ray diffraction experiment are reported in Table 1 and an ORTEP representation in Fig. 3. The X-structure reveals the presence of a coordinated acetonitrile molecule and one water molecule; $\nu_{\max}/\text{cm}^{-1}$ 3436 (OH), 1612 and 1576 (C–Carom), 1223 (CF), 1027 (SO). Elemental Anal. Calc. for $\text{C}_{23}\text{H}_{24}\text{CuF}_6\text{N}_4\text{O}_7\text{S}_2$ (MW 711.14): C, 38.85; H, 3.54; N, 7.88. Found: C, 38.78; H, 3.49; N, 7.91%.

2.9. Hydrolysis of BNPP catalyzed by copper complexes

In a typical kinetic experiment, 50 μl of a freshly prepared BNPP stock solution (20 mM) in buffer (50 mM MES for pH 5.38 and 6.24 and HEPES for pH 7.26) were added to 950 μl of same buffer containing copper(II) complex (**6** 50 μM ; **7** 100 μM) at 40 °C. Hydrolysis of BNPP was monitored by following the visible absorption change at 400 nm ($\epsilon = 18500 \text{ M}^{-1} \text{ cm}^{-1}$) due to the release of *p*-nitrophenolate anion (PNPate). Conversion from absorbance to concentration was performed by using the Lambert–Beer law (Eq. (1)). To take into account the concentration change of PNPate in function of pH, the $[\text{PNP}]_{\text{tot}}$ was calculated following Eqs. (1)–(4), where $\text{p}K_{\text{a}}$ of *p*-nitrophenol (PNP) is 7.15 [27]. The activity of the complex was determined in triplicate by the initial rate method.

$$[\text{PNPate}]_{\text{meas}} = \frac{\text{OD}}{18500} \quad (1)$$

$$[\text{PNPate}]_{\text{tot}} = [\text{PNPate}]_{\text{meas}} + [\text{PNP}] \quad (2)$$

$$\text{pH} = 7.15 + \log \frac{[\text{PNPate}]_{\text{meas}}}{[\text{PNP}]} \quad (3)$$

$$\begin{aligned} [\text{PNP}]_{\text{tot}} &= \left(1 + \frac{[\text{PNP}]}{[\text{PNPate}]_{\text{meas}}}\right) [\text{PNPate}]_{\text{meas}} \\ &= \left(1 + \frac{1}{10^{\text{pH}-7.15}}\right) \frac{\text{OD}}{18500} \end{aligned} \quad (4)$$

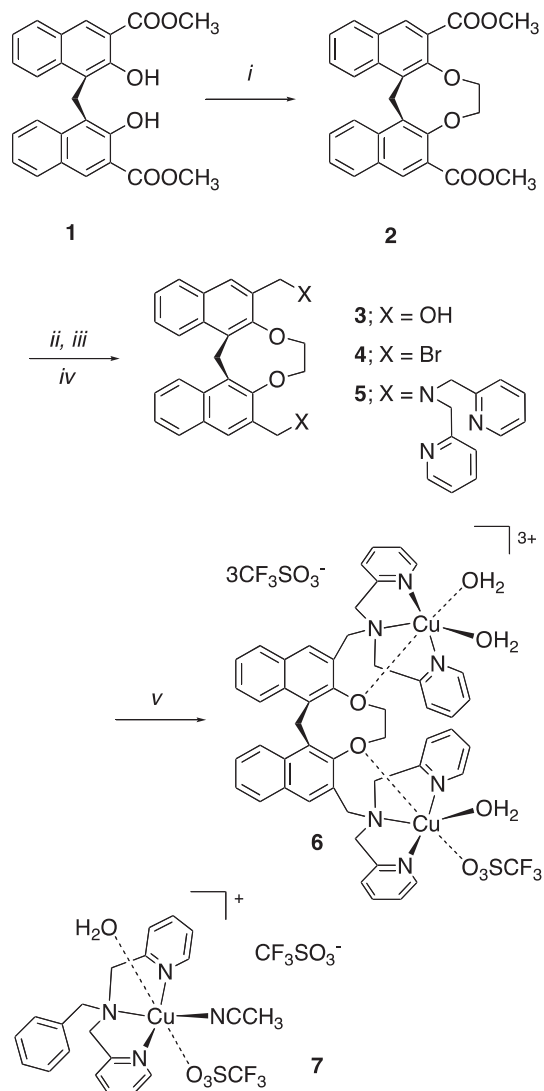
2.10. Crystallographic data

Single crystal X-ray diffraction data were collected on four circles Nonius Kappa-CCD diffractometer at 293 K, using monochromated Mo $K\alpha$ radiation, $\lambda = 0.71073 \text{ \AA}$. The structures were refined using SHELXL-97 [28]. H-atoms of water molecules complexed on copper ions of **6** were determined experimentally. One triflate anion in compound **6** was found to be strongly disordered and refined on several sites. The co-crystallized acetone molecule in this compound was also disordered and the oxygen was refined on 2 sites of occupancy equal to 0.5.

3. Results and discussion

3.1. Synthesis and characterization

The ligand **5** was synthesized in four steps from methyl pamoate **1** as described in Scheme 2. Methyl pamoate **1** was obtained by esterification in methyl alcohol of the commercially available pamoic acid [25]. As revealed by the X-ray structure (Fig. 1A), methyl pamoate **1** exhibits an important flexibility around the methano bridge linking the two naphthyl moieties that takes away the two ester groups. In order to rigidify the ligand skeleton and to constrain the ester groups in close vicinity, the compound **1** was transformed into the cyclic ether **2** by reaction with 1,2-dibromoethane in the presence of potassium carbonate in refluxing acetone. The poor yield (14%) in this step is nevertheless acceptable



Scheme 2. Synthesis of the ligand **5** and the Cu(II) complex **6** (reagents and conditions: (i) $(\text{CH}_2)_2\text{Br}_2$, K_2CO_3 , acetone reflux, 14%; (ii) AlLiH_4 , THF, 98%; (iii) PBr_3 , CH_2Cl_2 , 51%; (iv) BPA, diisopropylethylamine, ethyl acetate/ CH_2Cl_2 (1/1), 47% and (v) $\text{Cu}(\text{CF}_3\text{SO}_3)_2$, acetone, 90%).

since methyl pamoate **1** is cheap and the by-products of the reaction can be recovered. The cyclic ether **2** was reduced with LiAlH_4 into alcohol **3** and then transformed into the dibromo compound **4** by a bromination step using phosphorus tribromide. Compound **4** afforded suitable crystal for X-ray structure determination after recrystallized from chloroform. As expected, the 1,2-dioxoethano bridge linking the two naphthyl moieties maintains the bromomethane groups in a close vicinity and confers an envelop shape to the molecule (Fig. 1B). Finally, ligand **5** was prepared by N-alkylation of *N,N*-bis(2-picolyl)amine (BPA) of the dibromo compound **4** in the presence of *N,N*-diisopropylethylamine as base in a 1:1 mixture of ethyl acetate: CH_2Cl_2 as solvent.

The diCu(II) complex **6** was obtained in good yield by treatment of 1 equiv. of ligand **5** in acetone with 2 equiv. of copper(II) triflate. A deep blue powder was collected by filtration and single crystals suitable for X-ray structure determination were obtained by slow evaporation of a saturated solution of **6** in acetone at room temperature. Crystal data for complex **6**, together with details of the X-ray diffraction experiment are reported in Table 1 and selected bond lengths and angles in Table 2. In compound **6** one copper complex moiety is pointing inside the hydrophobic pocket, whereas the

Table 2
Selected bond lengths (Å) and angles (°) for **6**.^a

Cu(1) environment		Cu(2) environment	
<i>Bond lengths</i>			
Cu(1)–N(2)	2.008(3)	Cu(2)–N(5)	1.989(4)
Cu(1)–N(3)	1.990(3)	Cu(2)–N(6)	1.987(4)
Cu(1)–N(1)	2.019(3)	Cu(2)–N(4)	2.030(3)
Cu(1)–O(3)w	1.971(3)	Cu(2)–O(4)w	1.959(3)
Cu(1)–O(13)t	2.451(4)	Cu(2)–O(5)w	2.356(3)
Cu(1)–O(1)	2.593(3)	Cu(2)–O(2)	2.561(3)
<i>Angles</i>			
N(2)–Cu(1)–O(13)t	91.91(16)	N(5)–Cu(2)–O(5)w	87.29(16)
O(13)t–Cu(1)–N(3)	86.65(16)	O(5)w–Cu(2)–N(6)	89.74(15)
N(3)–Cu(1)–O(1)	88.73(14)	N(6)–Cu(2)–O(2)	89.91(14)
O(1)–Cu(1)–N(2)	93.82(14)	O(2)–Cu(2)–N(5)	93.59(14)
N(2)–Cu(1)–O(3)w	98.94(14)	N(5)–Cu(2)–O(4)w	98.84(18)
O(3)w–Cu(1)–N(3)	95.62(14)	O(4)w–Cu(2)–N(6)	95.28(18)
N(3)–Cu(1)–N(1)	83.14(14)	N(6)–Cu(2)–N(4)	83.42(15)
N(1)–Cu(1)–N(2)	82.35(14)	N(4)–Cu(2)–N(5)	82.75(15)
N(1)–Cu(1)–O(13)t	95.76(15)	N(4)–Cu(2)–O(5)w	92.84(14)
O(13)t–Cu(1)–O(3)w	85.25(14)	O(5)w–Cu(2)–O(4)w	92.54(15)
O(3)w–Cu(1)–O(1)	90.25(14)	O(4)w–Cu(2)–O(2)	85.22(14)
O(1)–Cu(1)–N(1)	88.63(14)	O(2)–Cu(2)–N(4)	89.39(14)

^a w and t stand respectively for water and triflate.

other is pointing outside the cavity (Fig. 2). The naphthyl-rings form a 79° angle and the Cu(1)–Cu(2) distance is 7.28 Å. Each copper ion shows a pseudo octahedral geometry with equatorial positions occupied by the three nitrogen atoms of BPA and a water molecule. Both copper(II) ions have an oxygen from the ether bridge in axial position, the sixth coordination being occupied by a triflate and a molecule of water for Cu(1) and Cu(2) respectively. The axial Cu–O distances (ranging from 2.36 to 2.59 Å) observed for both complexes are significantly longer than the equatorial ones and are relevant of a strong Jahn–Teller distortion. The equatorial angles sum is equal to 360.05° for Cu(1) and 360.29° for Cu(2) indicating no deviation from planarity. Due to the structure of BPA (one methyl group between amine and pyridines) constraint angles are present (between 82.59° and 83.64°) for N(3)–

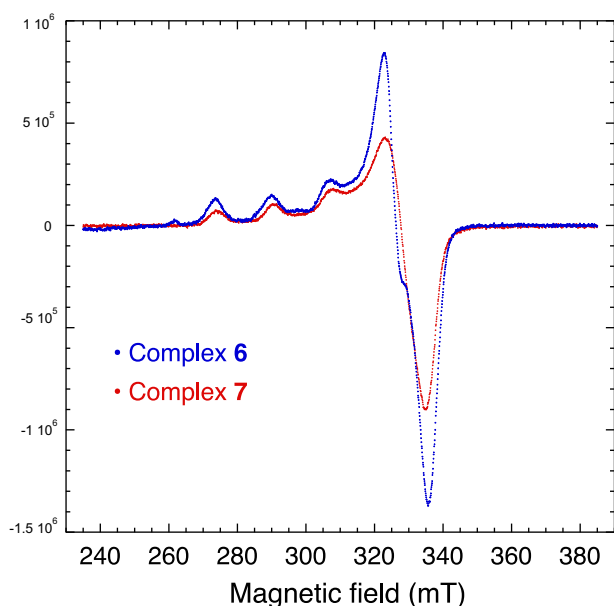


Fig. 4. ESR spectra of complexes **6** (blue) and **7** (red) in acetone. ESR conditions: 120 K, 9.445 GHz, microwave power 20 mW, modulation frequency 100 kHz, modulation amplitude 2G. (For interpretation of the references to color in this figure legend, the reader is referred to the web version of this article.)

Cu(1)–N(1), N(1)–Cu(1)–N(2), N(6)–Cu(2)–N(4), and N(4)–Cu(2)–N(5).

The mononuclear Cu(II) complex **7** was prepared in a similar fashion by treatment of 1 equiv. of *N*-benzyl-bis-2-picolyamine [26] in acetone with 1 equiv. of copper(II) triflate in good yield. A deep blue powder was collected by filtration and single crystals suitable for X-ray structure determination were obtained by slow evaporation of a saturated solution of **7** in acetone at room temperature (Fig. 3).

The X-band ESR spectra of **6** and **7** were recorded at 120 K in a frozen acetone solution (Fig. 4). The simulations with automatic parameter fitting were performed for axially symmetry environment and allowed us to get parameters corresponding to copper(II) environment ($g_{\parallel} = 2.264$, $g_{\infty} = 2.050$). The simulations with automatic parameter fitting were performed for axial symmetry environment and the obtained ESR constants are (hyperfine coupling constants expressed in $10^{-4} T$): complex **6**: $g_{\parallel} = 2.264$, $A_{\parallel} = 163.2$, $g_{\infty} = 2.057$, $A_{\infty} = 27.5$ and complex **7**: $g_{\parallel} = 2.260$, $A_{\parallel} = 161.5$, $g_{\infty} = 2.054$, $A_{\infty} = 16.7$. These constants are consistent with copper(II) ions in pseudo-octahedral geometries elongated along z-axis in accordance with the solid-state structures [29].

3.2. Phosphoesterase activity

The bis(*p*-nitrophenyl)phosphate (BNPP) hydrolysis was used to check the phosphoesterase activity of the copper complex **6**. Since, hydrolysis of BNPP by **6** proceeds cleanly to give *p*-nitrophenol (PNP) and *p*-nitrophenyl phosphate (MNPP) as revealed by thin-layer chromatography, the progress of the reaction was monitored by the visible absorbance change at 400 nm ($\epsilon = 18500 \text{ M}^{-1} \text{ cm}^{-1}$) due to the release of *p*-nitrophenolate anion (PNPate). The activity of the complex was determined by the initial rate method. The efficiency of the copper complex **6** was studied in the 7.26–5.38 pH range with respect to BNPP hydrolysis. Values of the observed initial rate for the appearance of PNPate are reported in Table 3 and in Fig. 5 as a function of the pH.

We observed first that no noticeable hydrolysis occurs without a copper complex in the 7.26–5.38 pH range (MES 50 mM for pH 5.38 and 6.24; HEPES 50 mM for pH 7.26; 10 min; 40 °C). While, complex exhibited a moderate catalytic activity at pH 6.24 and 7.26, it hydrolyzed rapidly BNPP at pH 5.38 (Fig. 5A). Unfortunately, the reaction stops after few minutes at 40 °C, probably due to an inhibition of the catalyst by the reaction product (MNPP). This phenomenon was already observed with other binuclear Cu(II) complexes for which an inactive μ -phosphato diCu(II) complex could be isolated [21]. Activity of complex **6** was compared to the one of complex **7**. The result is remarkable since the mononuclear Cu(II) complex **7** exhibited a poor activity in the same range of pH (Fig. 5B). The binuclear complex **6** is 41-fold more active ($V_{\text{obs}}^6/V_{\text{obs}}^7$) than the mononuclear one **7** (Table 3).

The kinetic of BNPP hydrolysis by complex **6** deserves some commentaries. First of all, the kinetic is not classical (Fig. 5A). The dependence of initial rate (V_{obs}) on the BNPP concentrations

Table 3
pH dependence of **6** vs. **7** in BNPP hydrolysis.^a

pH	Complex 6			Complex 7		
	V_{obs} ($\mu\text{M s}^{-1}$)	TON ^b	Conv. (%)	V_{obs} ($\mu\text{M s}^{-1}$)	$V_{\text{obs}}^6/V_{\text{obs}}^7$	
5.38	85 ± 3	11	24	2.09 ± 0.05	41	
6.24	13.8 ± 0.9	1.6	3	2.05 ± 0.09	7	
7.26	5.1 ± 0.1	1.2	2	1.99 ± 0.06	3	

^a Reaction conditions: [BNPP] = 2.25 mM; [**6**] = 50 M or [**7**] = 100 M; buffer = 50 mM (HEPES pH 7.26, MES pH 6.24 and 5.38); 40 °C.

^b $\text{TON} = [\text{BNPP}]_{\text{trans}}/[\text{6}]$.

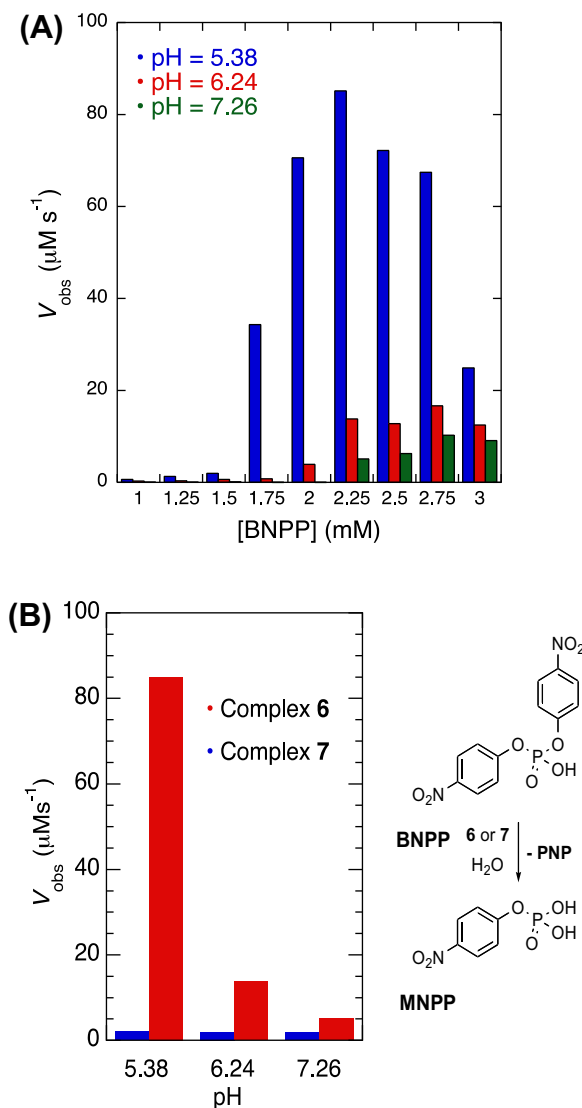


Fig. 5. (A) Plots of **6**-catalyzed BNPP hydrolysis initial rates vs. [BNPP] concentrations at 3 pH values (7.26, 6.24 and 5.38) and (B) pH dependence of complex **6** vs. **7** in BNPP hydrolysis (reaction conditions: [BNPP] = 2.25 mM; [**6**] = 50 μM or [**7**] = 100 μM ; buffer = 50 mM (HEPES pH 7.26, MES pH 6.24 and 5.38); 40 °C).

is not a hyperbolic curve as classically observed with other copper complexes [11] and complex **7**, but a sigmoid curve with a strong inhibition by the substrate at high BNPP concentrations. This behavior is generally encountered with allosteric enzymes that have multiple binding sites. In these cases, the affinity for ligand to one binding site is increased, upon the binding of ligand to another binding site [30]. Cooperativity is also observed in oligomeric proteins, when they undergo unfolding or unwinding during catalysis [31].

The second commentary regards the remarkable enhancement of the hydrolysis rate by **41** which clearly demonstrates a certain cooperativity between the two Cu(II) centers during the hydrolysis of BNPP. The X-ray structure of Cu(II) complex **6** revealed that Cu–Cu distance is about 7.287 Å, which is a too long distance to envisage a cooperativity between both copper(II) centers as depicted in Scheme 1 [3]. However, we can envisage that the binding of BNPP to the copper centers favors a conformational change which allows the shortening of the Cu–Cu distance to be compatible for a cooperativity in phosphate hydrolysis.

Another important feature of the copper(II) complex **6** is its maximum activity at pH 5.38. With another binuclear copper(II) complex, we observed a maximum of activity at pH 5.5–6 and we showed that a bis(aqua)copper complex is responsible for BNPP hydrolysis according to a double Lewis acid activation mechanism (Scheme 1) [11].

4. Conclusion

We described the synthesis and characterization of a new dinuclear Cu(II) complex **6** which exhibits a remarkable activity in the hydrolysis of activated phosphodiester BNPP with good conversion yields (24%) and TON (11). These results are very promising for the development of future more efficient metal catalysts for hydrolysis of phosphodiester.

Appendix A. Supplementary material

CCDC 655474, 655475, 655476 and 655477 contain the supplementary crystallographic data for compounds **1**, **4**, **6** and **7**, respectively. These data can be obtained free of charge from The Cambridge Crystallographic Data Centre via www.ccdc.cam.ac.uk/data_request/cif. Supplementary data associated with this article can be found, in the online version, at <http://dx.doi.org/10.1016/j.ica.2012.04.019>.

References

- [1] E.L. Hegg, J.N. Burstyn, *Coord. Chem. Rev.* 173 (1998) 133.
- [2] A. Sreedhara, J.A. Cowan, *J. Biol. Inorg. Chem.* 6 (2001) 337.
- [3] D.E. Wilcox, *Chem. Rev.* 96 (1996) 2435.
- [4] N. Mitic, S.J. Smith, A. Neves, L.W. Guddat, L.R. Gahan, G. Schenk, *Chem. Rev.* 106 (2006) 3338.
- [5] L.R. Gahan, S.J. Smith, A. Neves, G. Schenk, *Eur. J. Inorg. Chem.* (2009) 2745.
- [6] J.R. Morrow, O. Iranzo, *Curr. Opin. Chem. Biol.* 8 (2004) 192.
- [7] J.A. Cowan, *Chem. Rev.* 98 (1998) 1067.
- [8] G. Feng, E.A. Tanifum, H. Adams, A.C. Hengge, N.H. Williams, *J. Am. Chem. Soc.* 131 (1994) 12771.
- [9] J.-L. Tian, L. Feng, W. Gu, G.-J. Xu, S.-P. Yan, D.-Z. Liao, Z.-H. Jiang, P. Cheng, *J. Inorg. Biochem.* 101 (2007) 196.
- [10] B.K. Takasaki, J. Chin, *J. Am. Chem. Soc.* 116 (1994) 1121.
- [11] M.E. Branum, A.K. Tipton, S. Zhu, L. Que Jr., *J. Am. Chem. Soc.* 123 (2001) 1898.
- [12] C.A. Chang, B.H. Wu, C.-H. Hsiao, *Eur. J. Inorg. Chem.* (2009) 1339.
- [13] T. Koike, E. Kimura, in: A.G. Sykes (Ed.), *Advances in Inorganic Chemistry*, vol. 44, Academic Press, San Diego, CA, 1996, pp. 229–261.
- [14] T. Koike, M. Inoue, E. Kimura, M. Shiro, *J. Am. Chem. Soc.* 118 (1996) 3091.
- [15] P.U. Maheswari, S. Barends, S. Özalp-Yaman, P. de Hoog, H. Casellas, S.J. Teat, C. Massera, M. Lutz, A.L. Spek, G.P. van Wezel, P. Gamez, J. Reedijk, *Chem. Eur. J.* 13 (2007) 5213.
- [16] F. Verge, C. Lebrun, M. Fontecave, S. Ménage, *Inorg. Chem.* 42 (2003) 499.
- [17] A. Sreedhara, J.D. Freed, J.A. Cowan, *J. Am. Chem. Soc.* 122 (2000) 8814.
- [18] T. Gajda, Y. Düpre, I. Török, J. Harmer, A. Schweiger, J. Sander, D. Kuppert, K. Hegetschweiler, *Inorg. Chem.* 40 (2001) 4918.
- [19] A. Schiller, R. Scopelliti, K. Severin, *J. Chem. Soc., Dalton Trans.* (2006) 3858.
- [20] S. Sabiah, B. Varghese, N.N. Murthy, *Chem. Commun.* (2009) 5636.
- [21] K. Selmeçzi, M. Giorgi, G. Speier, M. Réglér, *Eur. J. Inorg. Chem.* (2006) 1022.
- [22] S. Negi, H.-J. Schneider, *Tetrahedron Lett.* 43 (2002) 411.
- [23] M. Zha, H.-L. Zhang, C. Zhao, L.-N. Ji, Z.-W. Mao, *Chem. Commun.* 47 (2012) 7344.
- [24] A. Rockenbauer, L. Korecz, *Appl. Magn. Reson.* 10 (1996) 29.
- [25] H. Fonge, S.K. Chitneni, J. Lixin, K. Vunckx, K. Prinsen, J. Nuyts, L. Mortelmans, G. Bormans, Y. Ni, A. Verbruggen, *Bioconjugate Chem.* 18 (2007) 1924.
- [26] S.-I. Kawahara, T. Uchimar, *Eur. J. Inorg. Chem.* (2001) 2437.
- [27] J.A. Dean, *Lange's Handbook of Chemistry*, 14th ed. McGraw-Hill (Table 8.8), New York 1992.
- [28] G.M. Shedrick, SHELXL-97, Program for Crystal Structure Refinement, University of Göttingen, Germany, 1997.
- [29] M. Schatz, M. Becker, F. Thaler, F. Hampel, S. Schindler, R.R. Jacobson, Z. Tyeklar, N.N. Murthy, P. Ghosh, Q. Chen, J. Zubieta, K.D. Karlin, *Inorg. Chem.* 40 (2001) 2312.
- [30] A. Cornish-Bowden, *Fundamentals of Enzyme Kinetics*, Portland Press, London, 1995.
- [31] M.F. Perutz, *Q. Rev. Biophys.* 22 (1989) 139.